

# Iterative Detection for Unique Word OFDM

Werner Haselmayr\*, Christian Hofbauer†, Bernhard Etlzinger\*, Andreas Springer\*, Mario Huemer†

\*Institute for Communications Engineering and RF-Systems, Johannes Kepler University, Linz, Austria  
{werner.haselmayr, bernhard.etzlzinger, andreas.springer}@jku.at

†Institute of Signal Processing, Johannes Kepler University, Linz, Austria  
{christian.hofbauer, mario.huemer}@jku.at

**Abstract**—In this paper we consider a unique word OFDM (UW-OFDM) system with iterative detection, for which we explore two soft-input soft-output (SISO) detection algorithms: A LMMSE detector and a detector based on the generalized approximate message passing (GAMP) algorithm. For the GAMP based detector we propose additional simplifications suitable for UW-OFDM to further reduce the complexity while exhibiting only a small BER performance loss. As verified by computer simulations, both algorithms show a significant BER performance improvement over the iterations. Moreover, the GAMP based detector with the proposed simplifications outperforms the computational more complex LMMSE detector.

**Index Terms**—GAMP, iterative detection, SISO LMMSE, UW-OFDM

## I. INTRODUCTION

Unique word - orthogonal frequency division multiplexing (UW-OFDM) is a novel signaling scheme [1], where the cyclic prefixes (CPs), used by classical OFDM signaling, are replaced by deterministic sequences, called unique words (UWs). In contrast to the CP, the UW can be designed to be used for particular receiver tasks, like channel estimation and/or synchronization<sup>1</sup>. Moreover, UW-OFDM achieves a better bit error rate (BER) performance than CP-OFDM for typical frequency-selective indoor scenarios [1]. However, this performance gain comes at the price of higher complexity: In classical CP-OFDM systems usually simple single-tap equalization is employed, whereas UW-OFDM requires more sophisticated detection schemes [2].

Recently, various linear and non-linear detection schemes were studied for uncoded and coded UW-OFDM in [2]–[6]. The investigations of the coded UW-OFDM systems were carried out by performing the detection and decoding task one-time. In this work we apply the concept of iterative detection to UW-OFDM, where reliability (soft) information is exchanged between a soft-input soft-output (SISO) detector and a SISO decoder [7], [8]. Since the generation of the UW introduces correlations among the subcarriers it is expected that the iterative approach provides a performance improvement compared to non-iterative detection. It is important to note that for classical CP-OFDM over time-invariant channels, iterative

detection provides no performance gain since no correlation among the subcarriers exists, i.e. no intercarrier interference<sup>2</sup> [9]. So far no SISO detectors suitable for UW-OFDM have been proposed and thus we close this gap and present two algorithms. Additionally, we provide simplifications for reduced complexity implementations. The main contribution of our work can be summarized as follows:

- We apply the concept of iterative detection to UW-OFDM. To the best of our knowledge no iterative approach has been considered for UW-OFDM systems.
- We present SISO detection algorithms, namely a linear minimum mean square error (LMMSE) detector and a detector based on the generalized approximate message passing (GAMP) algorithm. For the GAMP based detector we propose simplifications to further reduce the complexity. We show that valid simplifications are obtained for generator matrices (for UW-OFDM symbol generation) with approximately equal entries.
- We show through BER simulations, that for generator matrices with approximately equal elements the GAMP based detector, after several iterations, outperforms the LMMSE detector. Additionally, it also has a superior performance compared to UW-OFDM systems with a diagonal-like generator matrix, independent of the employed detector.

The paper is organized as follows: In Section II we introduce the UW-OFDM system, including the UW-OFDM symbol generation and the iterative detection. Section III introduces the SISO detection algorithms and the proposed simplifications. The BER performance of both algorithms when used in iterative detection and benchmarks are presented in Section IV. Finally, Section V concludes the paper.

*Notation:* We use lower-case bold face variables ( $\mathbf{a}$ ,  $\mathbf{b}$ , ...) to indicate vectors and upper-case bold face variables ( $\mathbf{A}$ ,  $\mathbf{B}$ , ...) to indicate matrices. The definition  $\text{diag}(\mathbf{a})$  is used for a diagonal matrix with the elements of vector  $\mathbf{a}$  on its diagonal and  $\mathbf{I}$  denotes the identity matrix. The transposition or conjugate transposition of a vector/matrix is denoted  $(\cdot)^T$  and  $(\cdot)^H$ , respectively. And the probability density function of a Gaussian random vector  $\mathbf{z}$  is fully described by its mean vector  $\boldsymbol{\mu}$  and covariance matrix  $\boldsymbol{\Sigma}$  according to  $\mathcal{N}_{\mathbf{z}}(\boldsymbol{\mu}, \boldsymbol{\Sigma}) \propto \exp(-(\mathbf{z} - \boldsymbol{\mu})^H \boldsymbol{\Sigma}^{-1} (\mathbf{z} - \boldsymbol{\mu}))$ , with  $\propto$  being the proportional operator.

Copyright (c) 2014 IEEE. Personal use of this material is permitted. Permission from IEEE must be obtained for all other uses, in any current or future media, including reprinting/republishing this material for advertising or promotional purposes, creating new collective works, for resale or redistribution to servers or lists, or reuse of any copyrighted component of this work in other works. DOI: 10.1109/GLOCOM.2014.7037309

<sup>1</sup>Nevertheless, the bandwidth efficiency of both approaches is approximately the same [1].

<sup>2</sup>However, in case of intercarrier interference, e.g. due to time-varying channels, iterative detection is often used for CP-OFDM.

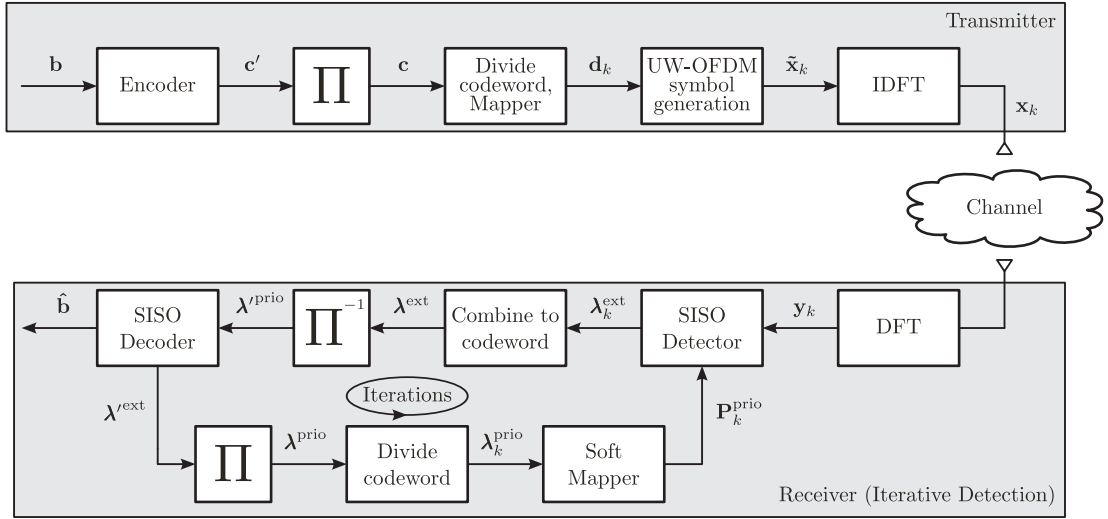


Fig. 1. UW-OFDM system with iterative detection. Note that the blocks  $\Pi$  and  $\Pi^{-1}$  denote the interleaving and deinterleaving process, respectively.

## II. UW-OFDM SYSTEM MODEL

We consider a coded UW-OFDM communication system as depicted in Fig. 1.

At the transmitter, a stream of information bits  $\mathbf{b}$  is encoded and interleaved yielding the codeword  $\mathbf{c}$ . For the transmission, the codeword  $\mathbf{c}$  is divided into  $K$  blocks of length  $QN_d$ , i.e.  $\mathbf{c} = [\mathbf{c}_1^T, \dots, \mathbf{c}_K^T]^T$  with  $\mathbf{c}_k = [c_{k,1}^T, \dots, c_{k,N_d}^T]^T$  and  $\mathbf{c}_{k,n} = [c_{k,n}^1, \dots, c_{k,n}^Q]^T$ . Each bit vector  $\mathbf{c}_{k,n}$  is mapped to a complex-valued symbol  $d_{k,n} \in \mathcal{S} = \{\alpha_1, \dots, \alpha_{2^Q}\}$  resulting in the symbol vector  $\mathbf{d}_k = [d_{k,1}, \dots, d_{k,N_d}]^T \in \mathbb{C}^{N_d \times 1}$ . The finite symbol alphabet  $\mathcal{S}$  contains  $M = |\mathcal{S}| = 2^Q$  symbols, and each symbol  $\alpha_i$  corresponds to a certain bit pattern  $\mathbf{s}_i = [s_i^1, \dots, s_i^Q]^T$ . The symbol vector  $\mathbf{d}_k$  is used for the generation of the  $k$ th UW-OFDM symbol, which is briefly reviewed in the following (for more details see [1]):

An UW-OFDM time domain symbol vector of length  $N$  shall be of the form  $[\tilde{\mathbf{x}}_k^T \mathbf{u}^T]^T$ , where  $\tilde{\mathbf{x}}_k \in \mathbb{C}^{(N-N_u) \times 1}$  is the information-bearing part affected by the data symbols. The vector  $\mathbf{u} \in \mathbb{C}^{N_u \times 1}$  denotes a predefined sequence at the tail of each OFDM time domain symbol vector which we call UW. W.l.o.g., this work only focuses on the case  $\mathbf{u} = \mathbf{0}$ , a UW different to the zero word can easily be obtained by a simple addition, cf. [10]. As in classical OFDM, the symbol vector  $\mathbf{d}_k$  and the zero subcarriers (usually at the band edges and at DC) are specified as part of the frequency domain vector  $\tilde{\mathbf{x}}_k$ . In addition UW-OFDM requires the zero-word to be specified in time domain as part of the vector  $\mathbf{x}_k = \mathbf{F}_N^{-1} \tilde{\mathbf{x}}_k$ .  $\mathbf{F}_N$  denotes the length- $N$ -DFT matrix with elements  $[\mathbf{F}_N]_{kl} = e^{-j\frac{2\pi}{N}kl}$  for  $k, l = 0, 1, \dots, N-1$ . The generation of the zeros in the time domain requires a certain level of redundancy in the frequency domain. For this purpose let us define a codeword  $\mathbf{a}_k \in \mathbb{C}^{(N_d+N_r) \times 1}$  with  $N_r = N_u$  by

$$\mathbf{a}_k = \mathbf{G} \mathbf{d}_k, \quad (1)$$

where  $\mathbf{G} \in \mathbb{C}^{(N_d+N_r) \times N_d}$  depicts a complex valued code generator matrix. Furthermore, the insertion of the zero subcarriers is modeled as  $\tilde{\mathbf{x}}_k = \mathbf{B} \mathbf{a}_k$ , where  $\mathbf{B} \in \{0, 1\}^{N \times (N_d+N_r)}$  consists

of zero-rows at the positions of the zero subcarriers, and of appropriate unit row vectors at the positions of occupied subcarriers. With these definitions the system of equations  $\mathbf{F}_N^{-1} \tilde{\mathbf{x}}_k = \mathbf{x}_k$  takes on the form  $\mathbf{F}_N^{-1} \mathbf{B} \mathbf{G} \mathbf{d}_k = [\tilde{\mathbf{x}}_k^T \mathbf{0}^T]^T$ . In order that the zero UW is generated for every possible data vector  $\mathbf{d}_k$ ,  $\mathbf{G}$  has thus to fulfill the constraint

$$\mathbf{F}_N^{-1} \mathbf{B} \mathbf{G} = \begin{bmatrix} * \\ \mathbf{0} \end{bmatrix}. \quad (2)$$

In non-systematically encoded UW-OFDM [11], the generator matrix takes on the form

$$\mathbf{G} = \mathbf{A} \begin{bmatrix} \mathbf{I} \\ \mathbf{T} \end{bmatrix}, \quad (3)$$

where  $\mathbf{A} \in \mathbb{R}^{(N_d+N_r) \times (N_d+N_r)}$  and  $\mathbf{T} \in \mathbb{C}^{N_r \times N_d}$ . Inserting (3) into (2) yields

$$\mathbf{F}_N^{-1} \mathbf{B} \mathbf{A} \begin{bmatrix} \mathbf{I} \\ \mathbf{T} \end{bmatrix} = \begin{bmatrix} * \\ \mathbf{0} \end{bmatrix}. \quad (4)$$

With  $\mathbf{M} = \mathbf{F}_N^{-1} \mathbf{B} \mathbf{A} = \begin{bmatrix} \mathbf{M}_{11} & \mathbf{M}_{12} \\ \mathbf{M}_{21} & \mathbf{M}_{22} \end{bmatrix}$ , where  $\mathbf{M}_{ij}$  are appropriate sized sub-matrices, the constraint in (4) is automatically fulfilled for any matrix  $\mathbf{A}$  by simply choosing  $\mathbf{T} = -\mathbf{M}_{22}^{-1} \mathbf{M}_{21}$ .

The matrix  $\mathbf{A}$  can be arbitrarily chosen and thus provides the degrees of freedom for an optimization of  $\mathbf{G}$  w.r.t. a specific cost function. In [11] the steepest descent algorithm has been utilized to find generator matrices that minimize the sum of the error covariances on the subcarriers after LMMSE detection in an additional white Gaussian noise (AWGN) scenario. For the AWGN case there exist infinitely many optimum generator matrices which all show the same performance. However, different initializations of  $\mathbf{A}$  in the steepest descent algorithm lead to different generator matrices which may then perform very differently in case of a multipath environment instead of AWGN. Two exemplary generator matrices are shown in Fig. 2. Whereas  $\mathbf{G}'$  distributes a data symbol mainly (however, not exclusively) locally and thus shows similarities to a classical OFDM system,  $\mathbf{G}''$  spreads the energy of a data symbol approximately uniformly over all

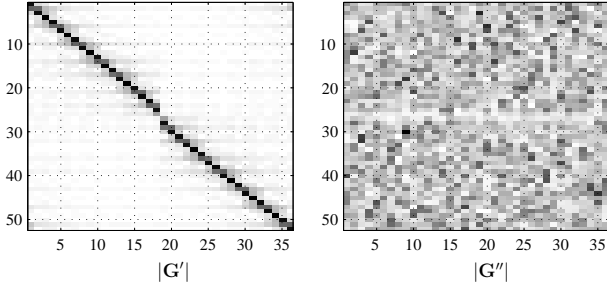


Fig. 2. Absolute values of the entries of exemplary generator matrices  $\mathbf{G}'$  and  $\mathbf{G}''$  with  $N_d=36$  and  $N_r=16$  [11]. The value increases with increasing darkness of the element.

subcarriers and thus behaves similar to a single carrier system.

Given an appropriate generator matrix, the  $k$ th transmit symbol in the time domain follows to

$$\mathbf{x}_k = \mathbf{F}_N^{-1} \mathbf{B} \mathbf{G} \mathbf{d}_k. \quad (5)$$

Consequently, the  $k$ th received UW-OFDM symbol in the frequency domain and hence our system model follows as

$$\mathbf{y}_k = \mathbf{H}_k \mathbf{G} \mathbf{d}_k + \mathbf{w}_k, \quad (6)$$

where  $\mathbf{H}_k \in \mathbb{C}^{(N_d+N_r) \times (N_d+N_r)}$  denotes the diagonal channel matrix which contains the sampled channel frequency response on its main diagonal, excluding the entries corresponding to zero subcarriers. The channel matrix  $\mathbf{H}_k$  originates from  $\mathbf{H}_k = \mathbf{B}^T \mathbf{F}_N \mathbf{H}_k^c \mathbf{F}_N^{-1} \mathbf{B}$ , where  $\mathbf{H}_k^c \in \mathbb{R}^{N \times N}$  denotes a cyclic convolution matrix with the zero-padded channel impulse response vector  $\mathbf{h}_k \in \mathbb{C}^{N \times 1}$  in its first column, and the noise vector  $\mathbf{w}_k \in \mathbb{C}^{N \times 1}$  follows a complex Gaussian distribution  $\mathcal{N}_{\mathbf{w}_k}(\mathbf{0}, \sigma^2 \mathbf{I})$ .

The SISO detector computes, based on the received signal  $\mathbf{y}_k$ , the channel state information ( $\mathbf{H}_k$  and  $\sigma^2$ ) and the *a priori* information from the decoder, the *extrinsic* log-likelihood ratios (LLRs)  $\lambda^{\text{ext}}(c_{k,n}^q)$  for each code bit  $c_{k,n}^q$  of the  $k$ th UW-OFDM symbol, which are collected in the vector  $\boldsymbol{\lambda}_k^{\text{ext}}$ . The LLRs of all UW-OFDM symbols are combined in the vector  $\boldsymbol{\lambda}^{\text{ext}}$ , that, after deinterleaving, is passed to the SISO decoder. The decoder computes *extrinsic* LLRs  $\boldsymbol{\lambda}^{\text{ext}}$ , which become *a priori* probabilities  $\mathbf{P}_k^{\text{prio}}$  after interleaving and soft mapping [8]. A cycle of feed back information from the decoder to the detector, followed by detection and decoding, is referred to as one iteration. If a maximum number of iterations is reached the channel decoder provides a hard-output estimate of the transmitted information bit stream  $\hat{\mathbf{b}}$ .

Throughout this paper, we assume perfect knowledge of the channel matrix  $\mathbf{H}_k$  and the noise variance  $\sigma^2$ . In what follows, we consider only a single UW-OFDM symbol and thus skip the index  $k$  (e.g.,  $\lambda^{\text{ext}}(c_{k,n}^q) \triangleq \lambda^{\text{ext}}(c_n^q)$ ).

### III. SOFT-INPUT SOFT-OUTPUT DETECTOR

The *extrinsic* LLRs are computed by the detector according to [12]:

$$\begin{aligned} \lambda^{\text{ext}}(c_n^q) &= \ln \frac{\sum_{\forall \alpha_i: s_i^q=0} p(\mathbf{y}|d_n = \alpha_i) \prod_{q' \neq q} P^{\text{prio}}(c_n^{q'} = s_i^{q'})}{\sum_{\forall \alpha_i: s_i^q=1} p(\mathbf{y}|d_n = \alpha_i) \prod_{q' \neq q} P^{\text{prio}}(c_n^{q'} = s_i^{q'})} \\ &= \ln \frac{\sum_{\forall \alpha_i: s_i^q=0} \exp\left(\frac{-|\alpha_i - m_n^{\text{ext}}|}{v_n^{\text{ext}}}\right) \prod_{q' \neq q} P^{\text{prio}}(c_n^{q'} = s_i^{q'})}{\sum_{\forall \alpha_i: s_i^q=1} \exp\left(\frac{-|\alpha_i - m_n^{\text{ext}}|}{v_n^{\text{ext}}}\right) \prod_{q' \neq q} P^{\text{prio}}(c_n^{q'} = s_i^{q'})}, \quad (7) \end{aligned}$$

where  $p(\mathbf{y}|d_n = \alpha_i)$  is the likelihood function and  $P^{\text{prio}}(c_n^q)$  denotes the *a priori* probability of each code bit  $c_n^q$ , which is included in the vector  $\mathbf{P}_k^{\text{prio}}$  (see Fig. 1). The sum over all symbols  $\alpha_i \in \mathcal{S}$ , for which  $s_i^q = 0$  and  $s_i^q = 1$  is denoted by  $\sum_{\forall \alpha_i: s_i^q=0}$  and  $\sum_{\forall \alpha_i: s_i^q=1}$ , respectively. The parameters  $m_n^{\text{ext}}$  and  $v_n^{\text{ext}}$  corresponds to the *extrinsic* mean and the *extrinsic* variance. For the computation of (7), we employ the SISO LMMSE detector and a detection algorithm based on generalized approximate message passing (GAMP), which are detailed in following.

#### A. SISO LMMSE Detector

For non-iterative detection it was shown in [2] that the LMMSE detector provides a good trade-off between performance and computational complexity. Thus, we consider the SISO LMMSE detector as a reference, and briefly summarize the SISO LMMSE detector in Tab. I for the system model in (6) based on the derivations in [12]. The algorithm is obtained by temporarily assuming  $d_n$  to be a Gaussian random variable [9], [12], completely described by the mean  $m_n^{\text{prio}}$  and variance  $v_n^{\text{prio}}$  (see Step 1). This may cause a performance loss (see Section IV) since the symbols  $d_n$  in (6) are originally taken from the discrete alphabet  $\mathcal{S}$ . The complexity of the LMMSE detector is mainly determined by the  $N_d \times N_d$  matrix inversion in (10) (see Step 2 in Tab. I) leading to the complexity  $\mathcal{O}(N_d^3)$ . Note that for classical CP-OFDM (10) reduces to the inversion of a diagonal matrix since  $\mathbf{G} = \mathbf{I}$ , leading to the well-known single-tap equalization.

#### B. SISO Detector based on the GAMP algorithm

We employ the sum-product GAMP algorithm [13], which is an approximation of the loopy belief propagation to compute MMSE estimates [9]. By providing several heuristic approximations, the GAMP algorithm enables a computational efficient way to compute the *extrinsic* parameters  $m_n^{\text{ext}}$  and  $v_n^{\text{ext}}$  without using a Gaussian assumption on the symbols  $d_n$ . This is illustrated by comparing Step 1 in Tab. II and Tab. I. The LMMSE detector directly approximates the prior probability  $P^{\text{prio}}$  as Gaussian distribution. In contrast, the GAMP approximates the *a posteriori* probabilities  $P^{\text{post}}$ , which accounts for discrete *a priori* probabilities  $P^{\text{prio}}$ . Note that the approximation of  $P^{\text{post}}$  is justified for strong correlations among the OFDM subcarriers and is based on the central limit theorem (see [14]). The GAMP algorithm is summarized in Tab. I for the system model in (6) based on the derivations in [13], [15]. In Step 2 and 4 of Tab. II we propose

TABLE I  
SISO LMMSE DETECTOR FOR UW-OFDM

- **Input**  $\{P^{\text{prio}}(d_n = \alpha_i), i = 1, \dots, M \text{ and } n = 1, \dots, N_d\}, \mathbf{H}, \mathbf{G}, \sigma^2$
- **Step 1** Compute *a priori* mean  $m_n^{\text{prio}}$  and variance  $v_n^{\text{prio}}$

$$m_n^{\text{prio}} = \sum_{i=1}^M \alpha_i P^{\text{prio}}(d_n = \alpha_i) \quad (8)$$

$$v_n^{\text{prio}} = \sum_{i=1}^M |\alpha_i - m_n^{\text{prio}}|^2 P^{\text{prio}}(d_n = \alpha_i). \quad (9)$$

- **Step 2** Compute *a posteriori* mean vector  $\mathbf{m}^{\text{post}}$  and covariance matrix  $\mathbf{V}^{\text{post}}$

$$\mathbf{V}^{\text{post}} = \left( \mathbf{V}^{\text{prio}}^{-1} + \frac{1}{\sigma^2} \mathbf{G}^H \mathbf{H}^H \mathbf{H} \mathbf{G} \right)^{-1} \quad (10)$$

$$\mathbf{m}^{\text{post}} = \mathbf{m}^{\text{prio}} + \frac{1}{\sigma^2} \mathbf{V}^{\text{post}} \mathbf{G}^H \mathbf{H}^H (\mathbf{y} - \mathbf{H} \mathbf{G} \mathbf{m}^{\text{prio}}), \quad (11)$$

with  $\mathbf{m}^{\text{prio}} = [m_1^{\text{prio}}, \dots, m_{N_d}^{\text{prio}}]^T$ ,  $\mathbf{V}^{\text{prio}} = \text{diag}([v_1^{\text{prio}}, \dots, v_{N_d}^{\text{prio}}])$ .

- **Step 3** Compute *extrinsic* mean  $m_n^{\text{ext}}$  and variance  $v_n^{\text{ext}}$

$$v_n^{\text{ext}} = \left( 1/v_n^{\text{post}} - 1/v_n^{\text{prio}} \right)^{-1} \quad (12)$$

$$m_n^{\text{ext}} = v_n^{\text{ext}} \left( m_n^{\text{post}}/v_n^{\text{post}} - m_n^{\text{prio}}/v_n^{\text{prio}} \right), \quad (13)$$

where  $m_n^{\text{post}}$  denotes the  $n$ th entry of the vector  $\mathbf{m}^{\text{post}}$  and  $v_n^{\text{post}}$  is the  $n$ th diagonal element of the matrix  $\mathbf{V}^{\text{post}}$ .

- **Output** Compute extrinsic LLR for each code bit  $c_n^q$  using (7)

additional simplifications suitable for the UW-OFDM system to further reduce the computational complexity. It can be seen that the most cumbersome operation is the computation of  $\mathbf{Z} = \mathbf{H} \mathbf{G}$ , leading to a complexity of  $\mathcal{O}(N_d^2)$ . Thus, we achieved a significant complexity reduction compared to the LMMSE detector. However, the GAMP algorithm requires inner iterations.

#### IV. SIMULATION RESULTS

The parameters of the simulated system are adapted to current wireless local area network (WLAN) standards and are as follows:  $N = 64$ ,  $N_d = 36$ ,  $N_r = N_u = 16$ , sampling frequency  $f_s = 20$  MHz, DFT period  $T_{\text{DFT}} = 3.2 \mu\text{s}$ , guard duration  $T_{\text{GI}} = 800$  ns. The index set of the zero subcarriers is  $\{0, 27, 28, \dots, 37\}$ . A convolutional encoder with rate  $1/2$ , constraint length 7 and the generator polynomial (133,171) is utilized as channel code, and QPSK serves as symbol alphabet  $\mathcal{S}$ . The presented simulation results are obtained by averaging over  $10^4$  channel realizations featuring an average delay spread of 100 ns. The channel impulse responses are modeled as tapped delay lines, each tap with uniformly distributed phase and Rayleigh distributed magnitude, and with power decaying exponentially. The channel instances are normalized to unit energy, for details we refer to [16].

The BER performance of the LMMSE detector and the GAMP based detector is depicted in Fig. 3 and Fig. 4, respectively. Note that for the GAMP based detector we use five inner iterations. We observed (results not shown in this paper) for both algorithms that the main performance gain is achieved between the first and the second iteration and no further improvement is obtained after the third iteration. Hence, we only consider the first and the third iteration.

TABLE II  
SISO DETECTOR BASED ON THE GAMP ALGORITHM FOR UW-OFDM

- **Input**  $\{P^{\text{prio}}(d_n = \alpha_i), i = 1, \dots, M \text{ and } n = 1, \dots, N_d\}, \mathbf{H}, \mathbf{G}, \sigma^2$
- **Initialization**  $\tau_{r_n}^{-1} = 0$ ,  $r_n = 0$  for  $n = 1, \dots, N_d$ , and  $\mathbf{u} = \mathbf{0}$ ,  $\mathbf{Z} = \mathbf{H} \mathbf{G}$  ( $z_{j,n}$  denotes the element of matrix  $\mathbf{Z}$  in the  $j$ th row and  $n$ th column)
- **Step 1** Compute mean  $m'_n$  and variance  $v'_n$

$$m'_n = \sum_{i=1}^M \alpha_i P^{\text{post}}(d_n = \alpha_i) \quad (14)$$

$$v'_n = \sum_{i=1}^M |\alpha_i - m'_n|^2 P^{\text{post}}(d_n = \alpha_i) \quad (15)$$

with

$$P^{\text{post}}(d_n = \alpha_i) = \frac{P_i}{\sum_{i'=1}^M P_{i'}} \quad (16)$$

and

$$P_i = P^{\text{prio}}(d_n = \alpha_i) \exp(-\tau_{r_n}^{-1} |\alpha_i - r_n|^2). \quad (17)$$

- **Step 2** Compute  $p_j$  and  $\tau_{p_j}$

$$\tau_{p_j} = \sum_{n=1}^{N_d} |z_{j,n}|^2 v'_n, \quad (18)$$

$$\mathbf{p} = \mathbf{Z} \mathbf{m}' - \Lambda_{\tau_p} \mathbf{u}, \quad (19)$$

with  $\mathbf{p} = [p_1, \dots, p_{N_d+N_r}]^T$ ,  $\mathbf{m}' = [m'_1, \dots, m'_{N_d}]^T$  and  $\Lambda_{\tau_p} = \text{diag}([\tau_{p_1}, \dots, \tau_{p_{N_d+N_r}}])$ .

If the all elements of  $\mathbf{G}$  are approximately equal, i.e.  $|g_{j,n}|^2 \approx \sum_{j,j,n} |g_{j,n}|^2 / ((N_d + N_r) N_d) = 1/(N_d + N_r)$ , the following simplification can be applied

$$\tau_{p_j} = \bar{v} |h_j|^2, \quad \text{with } \bar{v} = (N_d + N_r)^{-1} \sum_{n=1}^{N_d} v'_n, \quad (20)$$

where the  $j$ th diagonal element of  $\mathbf{H}$  is denoted by  $h_j$ . Note  $\bar{v}$  is different from  $\bar{v}$  defined in Step 2 for the LMMSE detection algorithm.

- **Step 3** Compute  $u_j$  and  $\tau_{u_j}$

$$\tau_{u_j} = (\sigma^2 + \tau_{p_j})^{-1} \quad (21)$$

$$\mathbf{u} = \Lambda_{\tau_u} (\mathbf{y} - \mathbf{p}), \quad (22)$$

with  $\Lambda_{\tau_u} = \text{diag}([\tau_{u_1}, \dots, \tau_{u_{N_d+N_r}}])$  and  $\mathbf{u} = [u_1, \dots, u_{N_d+N_r}]^T$ .

- **Step 4** Compute  $r_n$  and  $\tau_{r_n}$

$$\tau_{r_n} = \left[ \sum_{j=1}^{N_d+N_r} |z_{j,n}|^2 \tau_{u_j} \right]^{-1} \quad (23)$$

$$\mathbf{r} = \mathbf{m}' + \Lambda_{r_n} \mathbf{Z}^H \mathbf{u}, \quad (24)$$

where  $\Lambda_{r_n} = \text{diag}(\tau_{r_1}, \dots, \tau_{r_{N_d}})$ .

If  $|g_{j,n}|^2 \approx 1/(N_d + N_r)$  is fulfilled the following simplification can be applied

$$\tau_{r_1} = \dots = \tau_{r_{N_d}} = (N_d + N_r) \left[ \sum_{j=1}^{N_d+N_r} |h_j|^2 \tau_{u_j} \right]^{-1} \quad (25)$$

If the maximum number of iterations is not reached go to Step 1, otherwise continue with the Output step.

- **Output** Compute extrinsic LLR using (7) with  $v_n^{\text{ext}} = \tau_{r_n}$ ,  $m_n^{\text{ext}} = r_n$ .

Note, that in the first iteration no feed back from the decoder is available. As benchmarks we provide the performance of classical CP-OFDM, using the parameters in [1] (Table I), and the AWGN-bound, which is the performance of an UW-OFDM system over an AWGN channel. It is shown in Fig. 3 that UW-OFDM outperforms classical CP-OFDM. This is due

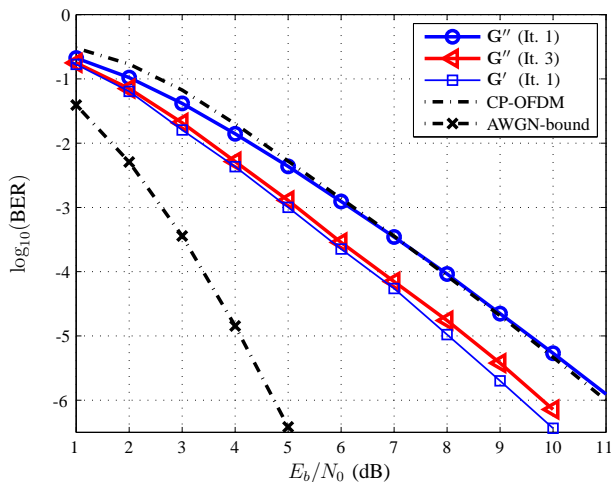


Fig. 3. Coded BER performance of an UW-OFDM system with LMMSE detector over several iterations.

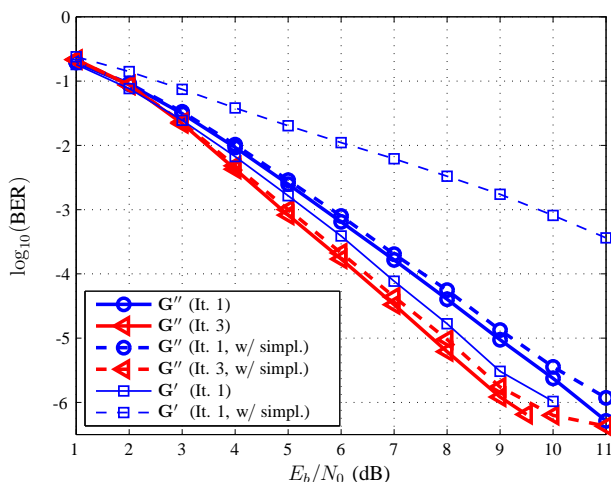


Fig. 4. Coded BER performance of an UW-OFDM system with a GAMP based detector over several iterations.

to fact that the preprocessing with  $G'$  or  $G''$  can be interpreted as a combination of precoding and inserting an additional level of redundancy that can be exploited at the receiver. However, a low rate channel code on top of  $G''$  provides only a low coding gain, while classical CP-OFDM achieves a high coding gain [11]. Thus, the difference between UW-OFDM with  $G''$  (no iteration) and CP-OFDM is small. Moreover it can be observed that the AWGN bound is not reached. This is due the severe channels, which are included in the  $10^4$  channel realizations that are generated for the simulations (also moderate fading channels). Similar observations have been made for severe intersymbol interference channels in [8]. The above discussion also holds for the GAMP based detector.

In Fig. 3 only the first iteration is depicted for  $G'$  since we observed no notable BER improvement over the iterations. This behavior comes from the fact that an UW-OFDM system with  $G'$  is similar to classical CP-OFDM, having its main elements located around the diagonal. With the matrix  $G''$  a significant improvement can be observed, achieving a performance gain between the first and the third iteration of 1.4 dB at  $\text{BER} = 10^{-6}$ . Similar to [11] it is shown that  $G'$  outperforms

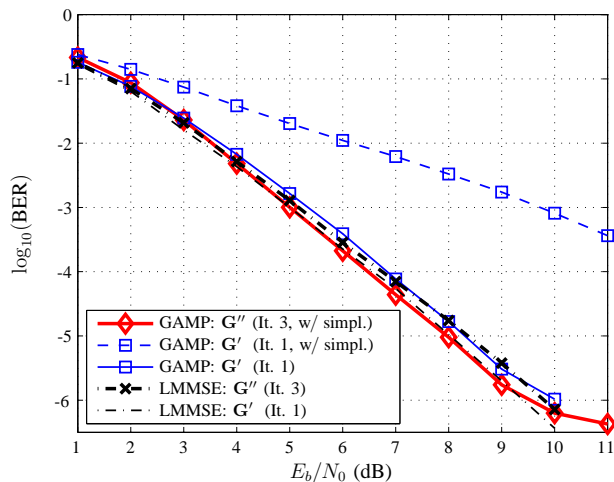


Fig. 5. Coded BER comparison between the LMMSE detector and the GAMP based detector.

$G''$ , when no iteration is employed. This is due to the fact that for low coding rates the coding gain for  $G'$  is higher than for  $G''$ . However, after three iterations the BER performance of an UW-OFDM system with  $G''$  is similar to a system using  $G'$ .

A similar behavior as for the LMMSE detector can be observed in Fig. 4 for the GAMP based detector. Additionally, the proposed simplifications only suffer a slight performance loss and the small error floor likely stems from the approximations made in the derivations of the GAMP algorithm (see [13] for more details.) In contrast to the LMMSE, the iterative system using  $G''$  outperforms the non-iterative UW-OFDM system with  $G'$ .

Note that the good BER performance of detectors on a system with  $G'$  without iterations is due to the fact that the UW-OFDM system appears to be similar to a classical CP-OFDM system. Such systems outperform single carrier systems (which are similar to UW-OFDM using  $G''$ ) for channel codes with low code rates.

Finally, Fig. 5 compares the LMMSE and the GAMP based detector. The proposed simplification for the GAMP algorithm (see Table II) only holds for generator matrices with approximately equal entries. Since the entries of  $G'$  are concentrated around the main diagonal, the simplification is not valid, resulting in a large performance loss. When not using the simplifications in the GAMP based detector, the LMMSE detector outperforms the GAMP detector for  $G'$ . This is due to the fact that the GAMP is derived with approximations that assume a strong correlation among the subcarriers which is not the case for the matrix  $G'$ . For  $G''$  the situation is different since the entries are approximately equal and thus the GAMP based detector performs better than the LMMSE detector.

## V. CONCLUSIONS

For an UW-OFDM system with iterative detection, we have proposed two SISO detection algorithms, namely a LMMSE detector and a GAMP based detector. For the GAMP based detector we have presented additional simplifications suitable for UW-OFDM to further reduce the computational complexity

while suffering only a marginal performance loss. Through computer simulations we were able to show that for the same generator matrix type the GAMP based detector, after several iterations, outperforms the LMMSE detector and an UW-OFDM system employing a diagonal-like generator matrix. This behavior was explained with the fact that a densely filled UW-OFDM generator matrix with approximately equal entries fulfills the assumptions made by the GAMP method. Thus, we conclude that for a generator matrix with approximately equal entries the GAMP algorithm with the proposed approximation should be applied, yielding a low-complexity algorithm with appealing performance.

#### ACKNOWLEDGMENT

This work has been partially supported by the Austrian COMET-K2 programme of the Linz Center of Mechatronics (LCM), and was funded by the Austrian federal government, the federal state of Upper Austria and by the Austrian Science Fund (FWF): I683-N13.

#### REFERENCES

- [1] M. Huemer, C. Hofbauer, and J. B. Huber, "The potential of unique words in OFDM," in *Proc. 15th Int. OFDM Workshop*, Hamburg, Germany, Sept. 2010, pp. 140–144.
- [2] A. Onic, "Receiver concepts for unique word OFDM," *Ph.D. Thesis, Alpen-Adria University Klagenfurt, Klagenfurt, Austria*, 2013.
- [3] M. Huemer, A. Onic, and C. Hofbauer, "Classical and Bayesian linear data estimators for unique word OFDM," *IEEE Trans. Signal Process.*, vol. 59, no. 12, pp. 6073–6085, Dec. 2011.
- [4] A. Onic and M. Huemer, "Sphere decoding for unique word OFDM," in *Proc. Conf. Global Telecommunications*, Houston, TX, USA, Dec. 2011, pp. 1–5.
- [5] M. Huemer, C. Hofbauer, A. Onic, and J. B. Huber, "On the exploitation of the redundant energy in UW-OFDM: LMMSE versus sphere detection," *IEEE Signal Process. Lett.*, vol. 19, no. 6, pp. 340–343, June 2012.
- [6] A. Onic, A. Schenk, M. Huemer, and J. B. Huber, "Soft-output sphere detection for coded unique word OFDM," in *Proc. 46th Asilomar Conf. Signals, Systems and Computers*, Pacific Grove, CA, USA, Nov. 2012, pp. 138–142.
- [7] C. Douillard et al., "Iterative correction of intersymbol interference: Turbo equalization," *Euro. Trans. Telecommun.*, vol. 6, no. 3, pp. 507 – 511, Sept.-Oct. 1995.
- [8] M. Tuechler et al., "Minimum mean squared error equalization using a priori information," *IEEE Trans. Signal Process.*, vol. 50, no. 3, pp. 673–683, Mar. 2002.
- [9] H. Wymeersch, *Iterative Receiver Design*. New York, NY: Cambridge University Press, 2007.
- [10] A. Onic and M. Huemer, "Direct vs. two-step approach for unique word generation in UW-OFDM," in *Proc. 15th Int. OFDM Workshop*, Hamburg, Germany, Sept. 2010, pp. 145–149.
- [11] M. Huemer, C. Hofbauer, and J. B. Huber, "Non-systematic complex number RS coded OFDM by unique word prefix," *IEEE Trans. Signal Process.*, vol. 60, no. 1, pp. 285–299, Jan. 2012.
- [12] Q. Guo et al., "A concise representation for the soft-in soft-out LMMSE detector," *IEEE Commun. Lett.*, vol. 15, no. 5, pp. 566 – 568, May 2011.
- [13] S. Rangan, "Generalized approximate message passing for estimation with random linear mixing," in *Proc. Int. Symp. Inf. Theory*, St. Petersburg, Russia, July 2011, pp. 2168–2172.
- [14] D. Donoho, A. Maleki, and A. Montanari, "Message passing algorithms for compressed sensing: I. motivation and construction," in *Proc. Inf. Theory Workshop*, Jan. 2010, pp. 1–5.
- [15] Q. Guo et al., "Iterative frequency domain equalization with generalized approximate message passing," *IEEE Signal Process. Lett.*, vol. 20, no. 6, pp. 559 – 562, June 2013.
- [16] J. Fakatselis, *Criteria for 2.4 GHz PHY Comparison of Modulation Methods. Document IEEE 1997; P802.11-97/157r1*, IEEE, Nov. 1997.